Eur Biophys J (2007) 36:199–211
DOI 10.1007/s00249-006-0120-4

ORIGINAL PAPER

External electric control of the proton pumping in bacteriorhodopsin

B. Povilas Kietis · Paulius Saudargas · György Vàró · Leonas Valkunas

Received: 4 May 2006 / Revised: 18 October 2006 / Accepted: 28 November 2006 / Published online: 21 December 2006

Abstract Comparative analysis of the photoelectric response of dried films of purple membranes (PM) depending on their degree of orientation is presented. Time dependence of the photo-induced protein electric response signal (PERS) of oriented and non-oriented films to a single laser pulse in the presence of the external electric field (EEF) was experimentally determined. The signal does not appear in the non-oriented films when the EEF is absent, whereas the PERS of the oriented PM films demonstrates the variable polarity on the microsecond time scale. In the presence of the EEF the PERS of the non-oriented film rises exponentially preserving the same polarization. The polarization of the PERS changes by changing the polarity of the EEF with no influence on the time constant of the PERS kinetics. The EEF effect on the PERS of the oriented films is more complicated. By subtracting the PERS when EEF $\neq$ 0 from the PERS when EEF = 0 the resulting signal is comparable to that of the non-oriented films. Generalizing the experimental data we conclude that the EEF influence is of the same origin for the films of any orientation. To explain the experimental results the two-state model is suggested. It assumes that the EEF directionally changes the $p\mathrm{K_a}$ values of the Schiff base (SB) and of the proton acceptor aspartic acid D85 in bacteriorhodopsin. Because of that the SB $\rightarrow$ D85 proton transfer might be blocked and consequently the L $\rightarrow$ M intermediate transition should vanish. Thus, on the characteristic time scale $\tau_{L \rightarrow M} \approx 30$ μs; both intermediates, the M intermediate, appearing under normal conditions, and the L intermediate as persisting under the blocked conditions when D85 is protonated, should coexist in the film. The total PERS is a result of the potentials corresponding to the electrogenic products of intermediates L and M that are of the opposite polarity. It is concluded that the ratio of bacteriorhodopsin concentrations corresponding to the L and M intermediates is driven by the EEF and, consequently, it should define the PERS of the non-oriented films. According to this model the orientation degree of the film could be evaluated by describing the PERS.

Keywords Photoelectric response · External electric field · Vectorial $p\mathrm{K_a}$ · Modeling of proton pumping

B. P. Kietis · P. Saudargas (✉) · L. Valkunas
Institute of Physics, Savanoriu 231,
02300 Vilnius, Lithuania
e-mail: saudargas@ar.fi.lt

B. P. Kietis
Department of Radiophysics, Faculty of Physics,
Vilnius University, Sauletekio 9, build. 3,
10222 Vilnius, Lithuania

L. Valkunas
Department of Theoretical Physics, Faculty of Physics,
Vilnius University, Sauletekio 9, build. 3,
10222 Vilnius, Lithuania
e-mail: valkunas@ktl.mii.lt

G. Vàró
Biological Research Center, Institute of Biophysics,
Szeged 7626, Hungary

Introduction

Bacteriorhodopsin (BR) is the simplest membrane protein functioning as an active proton pump in the purple membrane (PM) of *Halobacterium salinarum*

(Oesterhelt and Stoeckenius 1973). The light-induced proton transfer is driven by the retinal positioned inside the bundle of seven transmembrane helices and bound to residue Lys-216 via a protonated Schiff base (SB) (Mathies et al. 1991; Rotschild 1992; Lanyi 1993).

The structural organization of BR in the ground state and in the intermediate states is well determined, outlining the pathway and the initial steps of the proton translocation across the plasma membrane (Edman et al. 2004; Kimura et al. 1997; Essen et al. 1998; Luecke et al. 1999a, b; Belrhali et al. 1999; Lanyi 2000a, b, 2004a, b, c; Schobert et al. 2002; Brown et al. 2002; Neutze et al. 2002; Lanyi and Schobert 2002, 2003). Green light absorption triggers the proton pumping process resulting in redistribution of charges in the chromophore (Rousso et al. 1997) as a result of the *trans–cis* isomerization of the retinal, after its electronic excitation (Váró and Lanyi 1991). Subsequent proton translocation from the SB to the first acceptor D85 (corresponding to the $L \rightarrow M$ transition) is the key switch that is responsible for the unidirectional active proton transfer (Lanyi and Schobert 2002; Brown et al. 1998; Kandori 2004).

A photo-induced protein electric response signal (PERS) from bacteriorhodopsin was identified decades ago (Drachev et al. 1978; Hong and Montal 1979). PERS studies were performed on dried purple membrane samples (Lukashev et al. 1980; Váró and Keszthelyi 1983; Simmeth and Rayfield 1990), on BR incorporated in acrylamide gel (Dér et al. 1985; Ludmann et al. 1998), on BR proteoliposomes, on BR adsorbed to millipore filters (Hellingwerf et al. 1978), and on BR incorporated into planar lipid membranes (Bamberg et al. 1980; Braun et al. 1988). Initially the PERS in the oriented PM film results in a negative potential, which is opposite to the direction of active proton pumping, with subsequent changes into the positive potential, which might be attributed to the proton motive force. The time constant of this switching equals to ≈ 30 μs, which coincides with the time constant of the $L \rightarrow M$ transition (Groma et al. 2001). The M intermediate is commonly originated from the proton translocation from the SB to the initial proton acceptor D85. To emphasize the electrogenicity of this intermediate corresponding to the proton translocation further on we denote it as M^+. The characteristic time of the negative stage of the PERS coincides with the lifetime of the L intermediate. Thus, we will define this state as L^- by indicating that the potential of the electric polarity of the L intermediate is opposite to the proton pumping direction.

The $L \rightarrow M$ transition is sensitive to pH of the surrounding (Ludmann et al. 1998; Gergely et al. 1997). With decreasing pH, the originally purple protein discolors reaching the so-called ''acid-blue'' form at about pH3 (De Groot et al. 1990; Mowery et al. 1979; Váró and Lanyi 1989). At even lower pH values the color of BR again turns into purple in the presence of Cl^- or some other anions, thus, reaching the so-called ''acid-purple'' form (Mowery et al. 1979; Váró and Lanyi 1989; Fischer and Oesterhelt 1979). In the ''acid-blue'' form the M^+ intermediate is missing (Groma et al. 2001; Kobayashi et al. 1983; Chang et al. 1985; Ohtani et al. 1986; Chronister et al. 1986). The reason for that might be protonation of the acceptor D85 and, thus, resulting in the blockage of the proton transfer from the SB (Groma et al. 2001; Metz et al. 1992; Balashov et al. 1995, 1996; Wang 2000; Butt et al. 1989). As a result, the concentration of M^+ is reduced (Groma et al. 2001; Kietis et al. 2002, 2005). While the fact of D85 protonation under certain pH conditions is widely accepted, the proton donating group remains unidentified.

The influence of the external electric field (EEF) on the BR activity and possible regulation of the active proton pumping were studied by combining time-resolved spectroscopy and various electric measurements (Kietis et al. 2001a, b, c; Váró and Keszthelyi 1985; Kolodner et al. 1996, 1999; Lukashev et al. 1982). Common interpretation of the results obtained by using various approaches under different experimental conditions is based on the assumption that the EEF raises/reduces the energy barrier for the proton at the SB depending on the EEF polarity. Evidently, this variation originates in modification of the amplitude and/or time constant of the $L \rightarrow M$ transition (Kietis et al. 2001a, b, c, 2002, 2005; Váró and Keszthelyi 1985; Kolodner et al. 1996, 1999; Lukashev et al. 1982, 2001; Chamorovsky et al. 1983). This EEF influence is similar to the vectorial pH effect; thus, the influence of these external factors seems to be comparable (Kietis et al. 2001a; Kolodner et al. 2000). However, some questions still remain unanswered.

It has been demonstrated that the photocycle in dried PM films is interrupted in the M^+ intermediate when the relative humidity is <50%. Then the SB is reprotonated from D85 instead of conventional protonation from D96 (Groma et al. 2001). It is noteworthy that the rise time of the M^+ intermediate is much faster than its decay time. Thus, the maximal concentration of the M^+ intermediate in the dried film should correspond to the quasi-stationary conditions giving $M^+ = BR^*$, where BR^* is the number of the excited BR molecules and M^+ is the BR amount in the

M^+ state. With the assumption that M^+ increases in the presence of the EEF in the oriented PM film (Váró and Keszthelyi 1985; Lukashev et al. 2001) it might be possible to achieve the values $M^+ > BR^*$. However, any possible suggestion on how to obtain an increase of the concentration of the BR* in the presence of the EEF is not known so far.

The concentration of BR in the M^+ state either increases or decreases depending on the direction of the applied EEF. Two asymmetrical fractions of BR can be distinguished in the non-oriented films. Because of that the PERS might be generated in the non-oriented film in the presence of the EEF. Such kind of PERS was observed; however it was attributed to conductivity changes (Kietis et al. 2001a, b, c, 2002, 2005). The lack of experimental data of the non-oriented films inspired us to turn back to this problem.

To answer these questions the reasonable model describing the L → M transition should be used. Here, the physical model applicable to this transition stage will be presented. The basic statement of this model assumes that D85 in separate BR has to be either in the protonated or in the non-protonated state. Hence the two fractions of BRs with protonated and neutral D85 coexist in the same PM. The excited BR molecule with neutral D85 generating the positive potential on the extracellular side of the membrane determines the value of the M^+ concentration. The proton transfer from the SB in the BR with protonated D85 is blocked; thus, the molecule remains in the L^- state with the characteristic negative potential on the extracellular surface. The ratio of the BR fractions present in the PM generating potentials of the opposite polarity depends on the EEF. The model equation describing the L → M transition includes the concentrations of these fractions and the possible pathways of this unidirectional proton transfer. The single obstacle to this transfer is related to protonation of D85. The model is used to explain the PERS of the PM film of any orientation and the EEF effect, and demonstrates the possibility to estimate the orientation magnitude of a particular dried PM film.

Materials and methods

Sample preparation Non-oriented films of PM of *Halobacterium salinarum* were produced by drying the PM suspension on an indium-tin-oxide (ITO) conducting glass plate; hence the orientation of the individual PM in such a film is random. Oriented PM films were electrophoretically precipitated on a glass plate coated with the same ITO layer according to the standard procedure (Váró and Keszthelyi 1983; Váró 1981). Intracellular side of the PM is directed towards the ITO electrode, which is used as the ground electrode in the oriented films (see Fig. 1). Hence the proton transfer is directed towards the measuring electrode. The ITO layer served as a light-transparent electrode for measuring the optical density and the photoelectric potential of the film. The area of the film surface is 0.5 cm^2 in size. The optical density of the film was ≈2 optical units and correspondingly the thickness was estimated to be ≈14 μm.

External pH conditions of the films were varied by soaking the sample for 2 min in 1 M HCl solution reaching the so-called acidic conditions and afterwards dried in the air. It is noteworthy that the acidification effect is reversible. The relative humidity of the environment was about 50%.

Photoresponse Second harmonics (532 nm) of the Q-switched Nd:YAG laser was used for the optical excitation of the sample. The energy of the excitation light pulse was ≈10 mJ, the pulse duration ≈3 ns. The PERS was defined by using a home built setup, schematically shown in Fig. 1. The voltage generated by the light pulse depends on the orientation degree of the PM in the film. The PERS experimental results were obtained by averaging 50 separate photoresponses.

To explore the influence of the EEF the external potential was applied to the film through the 1.5 GΩ resistor (see Fig. 1). The EEF could possibly induce

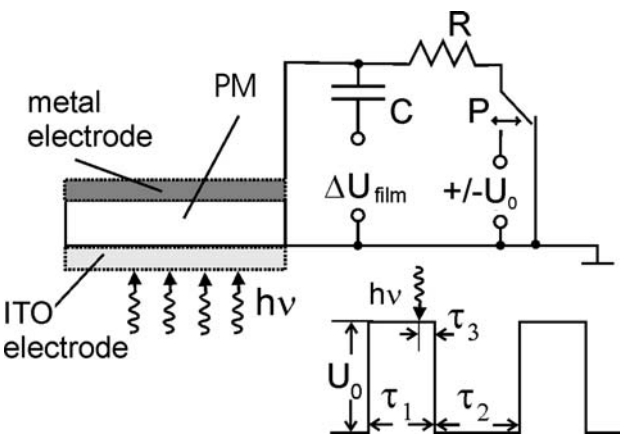

Fig. 1 Experimental scheme describing the photoresponse studies. The dried PM film serves as a dielectric medium between two electrodes, the metal (*above*) and the light transparent ITO conducting glass (*below*). *R* is an external resistor which was chosen to be 1.5×10^9 Ω and $+/-U_0$ determines the bias electric potential that is applied to the sample by means of the electrical switch *P*. The pulse duration of U_0 is indicated as τ_1 ≈1 s, the time period between the pulses is τ_2 ≈5 s, and τ_3 ≈0.2 s. ΔU_{film} indicates the electric potential generated by light in the film, while the external capacitor *C* of 100 pF cuts off the constant bias potential

the ion injection from the contact area causing the effect similar to the pH influence; therefore the EEF was applied temporarily for 1 s avoiding cumulative polarization of the sample. As the resistance of the sample did not exceed $R_{film} \approx 10^{12}$ Ω, and the capacitance was $C_{film} \approx 10^{-11}$ F; hence the characteristic time of the charge transit was $\tau_{tr} = C_{film} \cdot R_{film} \approx 10$ s. A detailed description of the PERS measurement is presented elsewhere (Kietis et al. 2001a, b, c, 2002, 2005).

Experimental results

In the absence of the EEF the total proton pumping potential in the non-oriented films is zero ($\Delta U_{film} = 0$). This is why the non-oriented films were considered to be not suitable for the electrical studies so far. However, the PERS of the non-oriented films appears if the external electric potential is applied. Kinetics of the PERS of the non-oriented film for different external potential values is shown in Fig. 2a. The negative external potential (the EEF is applied along the measuring direction) generates a positive electric signal and vice versa. The experimental kinetics of the PERS shown in Fig. 2a is single-phase; therefore, it can be well characterized by a single exponential:

$$\Delta U_{film} = U^0_{film}\left[1 - \exp\left(\frac{-t}{\tau_{film}}\right)\right], \quad (1)$$

indicating its relaxation character with the time constant of tens of microseconds. The amplitude of the PERS, ΔU_{film_max}, linearly depends on the EEF in both voltage polarity regions ($\theta_1 = \theta_2$) as is demonstrated in Fig. 2b. The PERS of a non-oriented PM film disappears at low pH (<pH3).

As is well known the PERS from the oriented film persists even in the absence of the EEF. It contains two phases, a fast negative signal is followed by a slower positive one with a transition time constant of ~30 μs. Typical kinetics of the PERS for the oriented PM film is shown in Fig. 3a.

The PERS of the well-oriented PM film under low pH conditions (see also, for instance Groma et al. 2001) contains only the first component (fast negative), which is independent of the value of the applied external electric field (Fig. 3a). The positive electric potential, attributed to the proton movement in the films at low pH, is absent, while the pathways of the active proton transfer are blocked (see Discussion).

At normal pH, the amplitude of the positive phase of the PERS depends on the external electric potential U_0 as shown in Fig. 3a. The PERS at the zero external electric field was subtracted from the PERS signals at different EEF values to distinguish the pure EEF effect, and the results defined as $\Delta(\Delta U_{film}) = \Delta U_{film(U_0 \neq 0)} - \Delta U_{film(U_0=0)}$ are presented in Fig. 3b. The PERS amplitude ΔU_{film_max} is dependent on the polarity of the EEF ($\theta_1 \neq \theta_2$) as is demonstrated in Fig. 3c. The EEF oriented oppositely to the measuring direction creates the positive external potential, while the ITO electrode is chosen to be the ground electrode (see Fig. 1). Thus, the PERS is reduced with the EEF if the positive potential is applied. Presumably the negative potential should produce the inverse effect; however, with a smaller amplitude (see Fig. 3b). The relevant explanation of this asymmetric EEF effect is given in Discussion.

Similar attempts to demonstrate the effect of the EEF on the photoelectric signals were already presented (Kietis et al. 2001) but under different experimental conditions, i.e. the resistance of the films determined descending kinetics on the microsecond time scale while in our case the high resistance films produce the growing potential on the same time scale.

Discussion

The L → M transition in BR, which is the first step from the sequence of steps in the proton transfer pathway in the photocycle, evidently determines the PERS of the oriented (Fig. 3) and the non-oriented (Fig. 2) films. Therefore, we will employ a two-state model for description of the experimental observations. According to this model the EEF should modulate the energy barrier between the two states corresponding to the proton alocation (Váró and Keszthelyi 1985) and/or evoke changes of the population of the first proton acceptor D85. The latter is caused by the presence of other proton accepting/donating groups in the protein and in the environment, similar to the case of the ion transition through channels (Chizmadjev and Aityan 1977). Evidently, the first proton acceptor D85 can be either free or occupied (protonated) depending on pH or due to the EEF. If the proton acceptor D85 is protonated the proton transfer between the two states is suspended. The comparative analysis of the experimental data of the oriented and the non-oriented films lets us to conclude that the protonation of the acceptor D85 is the dominant factor of the proton transfer in BR.

First let us discuss briefly the possible variability of the barrier height depending on the orientation of the EEF. Evidently, the variability of the barrier height would change the time constant of the L → M transi-

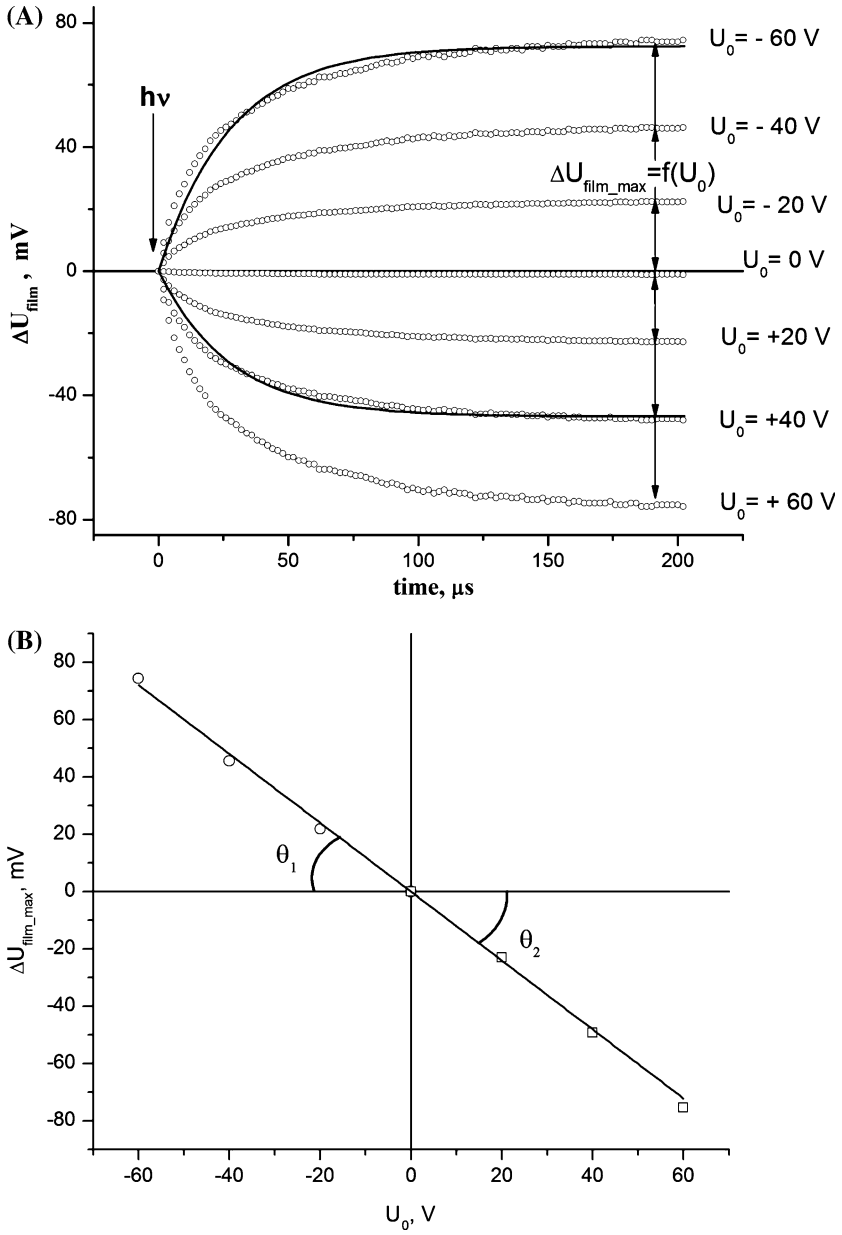

Fig. 2 Photoresponse ΔU_{film} of the non-oriented PM film in the presence of the EEF. Values of the bias electric voltage U_0 used for measurements are indicated in **a**. The theoretical curves calculated according to Eq. 14 at $U_0 = -60$ V and $U_0 = +40$ V (*solid lines* (**a**)) with the following parameters $\tau_L = 33$ μs, and $k\text{BR}^* \gamma = 1.2 \times 10^{-3}$. The amplitude of the PERS $\Delta U_{\text{film}\backslash\_\backslash\text{max}}$ depends on the external electric potential U_0 antisymmetrically (**b**). The angles between the linear fit lines of the experimental data obtained for the negative/positive external potentials U_0 and the *X*-axis are indicated as θ_1 and θ_2, respectively

tion (Váró and Keszthelyi 1985; Läuger et al. 1981). Thus, for characterization of the non-oriented films two different PM fractions of the opposite orientation and, therefore, characterised by two different time constants, should be suggested. Let us define the time constant corresponding to the transition between the two states (the decay time of the L^- state) as $\tau_{\overrightarrow{L}}$ for the fraction where the EEF and proton pumping directions coincide and $\tau_{\overleftarrow{L}}$ in the opposite case. The PERS of such a non-oriented film whould be determined as a difference of the two PERSs corresponding to the oriented films of separate fractions. Thus, by using the single-exponential description for each fraction (Läuger et al. 1981) the resultant PERS can be given by:

$$\Delta U_{\text{film1}} - \Delta U_{\text{film2}} = k\text{BR}^* \left[\exp\left(\frac{t}{\tau_{\overrightarrow{L}}}\right) - \exp\left(\frac{t}{\tau_{\overleftarrow{L}}}\right) \right], \tag{2}$$

where k is the proportion coefficient matching the dimensions. Within the frame of such description the variability of the decay times is up to 30% at the maximal values of the EEF (Váró and Keszthelyi 1985), thus, by assuming that $\tau_{\overrightarrow{L}} = 35$ μs and $\tau_{\overleftarrow{L}} = 25$ μs the function defined by Eq. 2 has its maximum at $t_{\max} = 30$ μs. This function equals to zero ($\Delta U_{\text{film}} \approx 0$) at the begining ($t = 0$ μs) and approaches zero at the end of the L → M conversion ($t = 200$ μs) as shown in

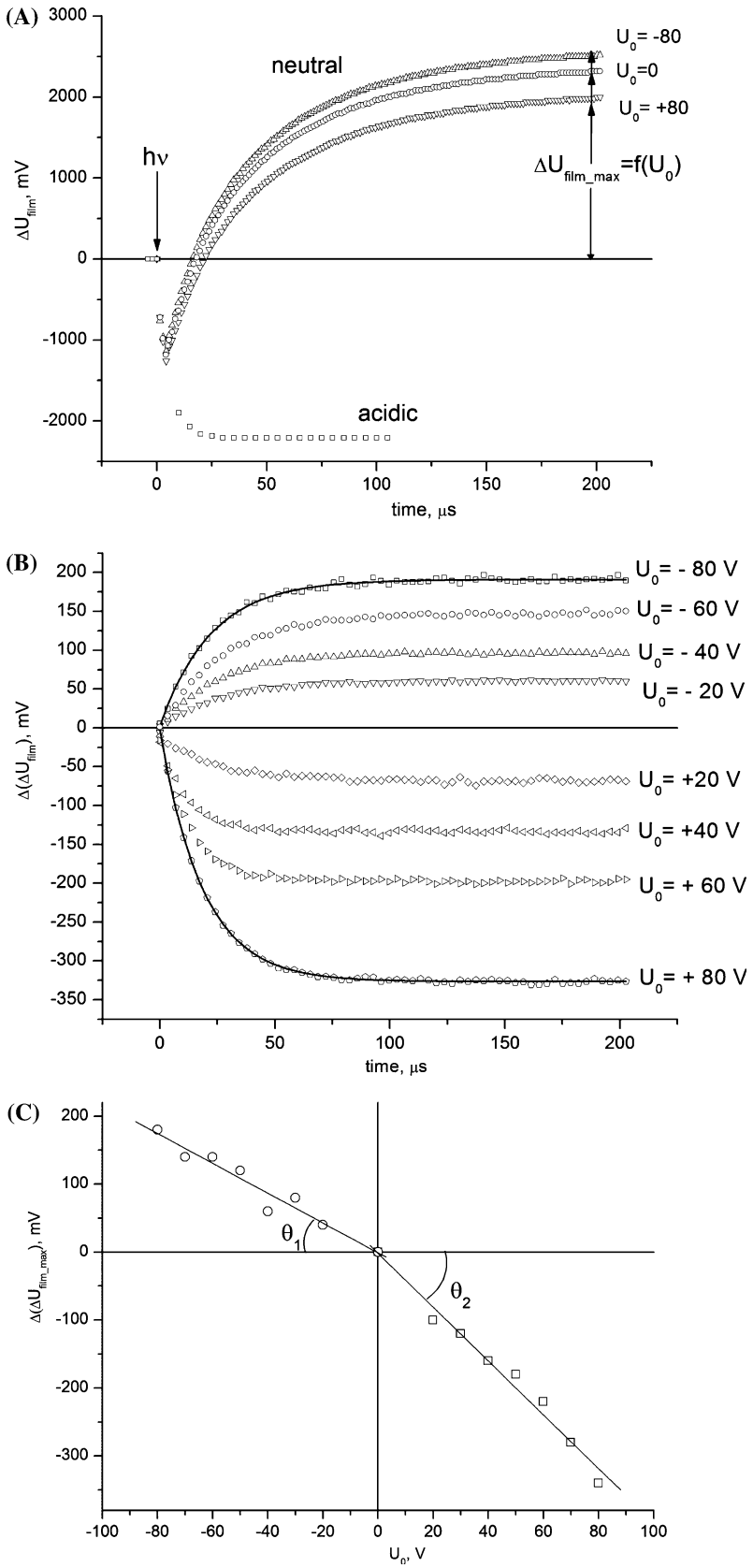

Fig. 3 Experimental results of the photoresponse ΔU_{film} after light excitation of the oriented dried PM film under normal conditions are presented in **a**: *circles* correspond to U_0 = 0 V; *triangles up* to U_0 = –80; *triangles down* to U_0 = + 80 V, and *squares* to the samples under low pH conditions. The PERS of an oriented film under low pH conditions does not depend on the EEF applied. The difference of the PERS of the oriented film when EEF ≠ 0 and when EEF = 0 is presented in **b**. The amplitude of the positive part of the PERS ΔU_{film_max} depends on the external electric potential U_0 (**c**). The effect of the EEF is not symmetrical, i.e. the positive external potential affects the amplitude of the response more than the negative one when the EEF is oriented along the measuring direction. The angles between lines of the linear fit of the experimental data obtained for the negative/positive external potentials U_0 and the *X*-axis are indicated as θ_1 and θ_2, respectively

Fig. 4. However, it is not the case in the experimental observations presented in Figs. 2 and 3 and Eq. 2 does not coincide with Eq. 1. Thus, the variability of the proton population of the final state of the two-state model will be considered as the dominant factor in developing the model.

External blockage of the proton pumping

To describe the proton movement along a particular one-dimensional pathway as is the case in BR (Grudinin et al. 2005), the Grotthuss model can be applied. The same concept is used to describe the ion movement in biological channels and in carbon nanotubes (Zhu and Schulten 2003). To describe the blockage possibility of a particular step of the proton transfer (Chizmadjev and Aityan 1977) the occupation factor ϑ should be introduced. The occupation factor $\vartheta = 0$ if the site is vacant and $\vartheta = 1$ if the site is occupied. Hereinafter we use the occupation factors constructing the two-state model.

The specific electrogenic properties of the L → M reaction have already been discussed (Kietis et al. 2001). For further discussion we will use the modified version of the two-state model of the proton transfer (Kietis et al. 2001). The potential energy barrier of the hydrogen bond between the SB and D85 decreases upon light excitation as a result of a piezoelectric feature of the medium (Kietis et al. 2001a, b) and due to the corresponding polarization electric field. Thus the appropriate conditions for the activation type of the proton transfer are established in the L^- intermediate. The pK_a values of the active residues change, subsequently creating the donor–acceptor pathway for the proton transfer. The internal electric field of the polarization origin probably implements these changes of pK_a. When the proton transfer SB → D85 is fulfilled, the polarization vanishes due to release of the mechanical strains, while the electric field of the opposite direction created by the energized proton persists.

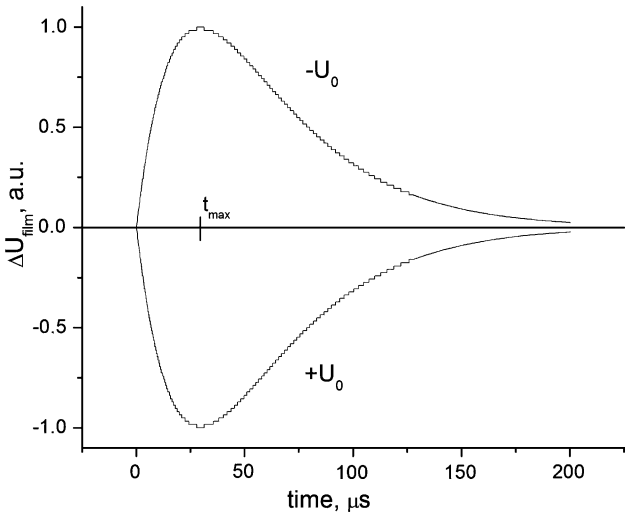

Fig. 4 Theoretical PERS of a non-oriented PM film calculated according to Eq. 2, under the assumption that the EEF influences only the energy barrier between the SB and D85, also the time constant of the L → M transition is changed (Váró and Keszthelyi 1985; Zhu and Schulten 2003). The time constants were chosen to be $\tau_{L}^{-} = 35\,\mu s$ (if the EEF and the proton pumping directions coincide) and for the opposite fraction $\tau_{L}^{+} = 25\,\mu s$, which corresponds to ±15% of the time constant of a normal L → M transition corresponding to the zero EEF. The function has its maximum at $t_{max} = 30$ μs. The presented *two curves* correspond to the opposite polarities of the external voltage applied

The PERS is a result of the sequential conversion between the intermediates $BR^* \longrightarrow \tau_0 L^- \longrightarrow \tau_L M^+$ due to difference in their electrogenicity. Since the time constant of the L^- decay, τ_L, is much larger (tens of micro-seconds) than the value of all primary events, τ_0 (a few micro-seconds), then the following relationship well describes the amount of the electrogenic intermediate L^-:

$$\frac{dL^-}{dt} = -\frac{L^-}{\tau_L}. \tag{3}$$

Taking into account the occupation factors of the possible proton binding sites the time constant can be given by:

$$\tau_L = \frac{1}{\upsilon_0 \vartheta_{SB}(1-\vartheta_{D85})} \exp\left(\frac{W_L}{kT}\right), \tag{4}$$

where υ_0 is the proton oscillation frequency in the initial state; W_L is the energy barrier for the SB → D85 transition; ϑ_{SB} and ϑ_{D85} define the occupational factors of SB and D85, respectively. The occupation factor of the SB $\vartheta_{SB} = 1$ and that of the acceptor $\vartheta_{D85} = 0$ correspond to the normal conditions when the proton is positioned in the initial state and the time constant is $\tau_L \approx 3 \times 10^{-5}$s. We define this state as a normal state, indicating it as BR_N.

The proton transfer is completed since the time constant of the electric signal measurement is $\tau_{obs} > 3 \times 10^{-4}$s. The subsequent proton transfer processes are stopped in the dried films (Groma et al. 2001), hence the momentary amounts meet the following relation:

$$BR^* = L^-(t) + M^+(t). \tag{5}$$

The PERS resulted from these intermediates can be defined as:

$$\Delta U_{\text{film}} = k(M^{+}(t) - L^{-}(t)), \tag{6}$$

where k is the proportion coefficient matching the dimensions. From Eqs. 3 and 6 under the initial conditions when $L^{-} = \text{BR}^{*}$ we get:

$$\Delta U^{N}_{\text{film}} = k \cdot \text{BR}^{*}_{N\uparrow\uparrow}\left[1 - 2\exp\left(-\frac{t}{\tau_L}\right)\right], \tag{7}$$

where $BR^{*}_{N\uparrow\uparrow}$ is the amount of the neutral (under normal pH conditions) excited BR molecules. Subscript N outlines the neutral state of the molecule. The first arrow in the subscript indicates the measuring direction, and the second arrow corresponds to the direction of the proton pumping (see Fig. 6 for details). It is worthwhile to mention that for highly oriented samples both directions coincide.

At low pH of the environment the proton acceptor D85 is protonated (Groma et al. 2001; Gergely et al. 1997; Váró and Lanyi 1989; Kobayashi et al. 1983); thus $\vartheta_{D85} = 1$. Hence from Eq. 3 we get that $\tau_L = \infty$, and further we indicate such ''acidic'' state as BR_{A}, and the resultant PERS equals to:

$$\Delta U^{A}_{\text{film}} = -k \cdot \text{BR}^{*}_{A\uparrow\uparrow}, \tag{8}$$

where $\Delta U^{A}{}_{\text{film}}$ represents the response of the ''acidic'' film and $BR^{*}{}_{A} \uparrow \uparrow$ is the amount of the excited BR molecules under the acidic conditions. The previous analysis describes the protonation of the acceptor D85 by the proton density under low pH conditions; however, the same effect can also be obtained by the EEF as it will be demonstrated in the following section.

BR molecule in the external electric field

This model of the proton pumping is based on the assumption that $\text{p}K_{\text{a}}$ of the proton acceptor D85 in the L intermediate increases in comparison with the SB as a result of the piezoelectric field. The EEF effect is analogous to the influence of the piezoelectric field; thus, D85 should experience the same effect under the EEF influence. Therefore, in the presence of the EEF the acceptor D85 can be protonated from the external side of the membrane. The energy diagram of this process is shown schematically in Fig. 5. The R82 seems to be associated with the proton release pathway, (Balashov et al. 1996; Imasheva et al. 1999) and should also control the $\text{p}K_{\text{a}}$ of D85, (Imasheva et al. 1999); hence it could also be involved in the proton donating group when D85 is protonated as a result of the EEF influence or under low pH conditions. However, there is no direct evidence, which group plays the main role in the proton donation; thus, we denote it as ''X'' as shown in Fig. 5.

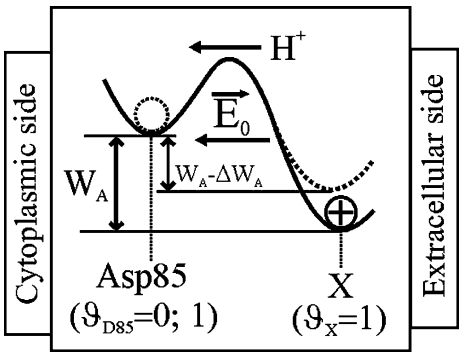

Fig. 5 The scheme of the potential energy surfaces of the proton positioning between D85 and possible proton donating group X. *Solid line* corresponds to the ground state of BR. In the ground state X is protonated and the potential well at D85 is unoccupied, hence the occupational factors are: $\vartheta_{D85} = 0, \vartheta_X = 1$ under neutral pH conditions. The EEF $\vec{E}_0$ of the proper direction and strength should change $\text{p}K_{\text{a}}$ of these two residues, subsequently reducing the energy difference W_A between two states by the value ΔW_A (*dotted line*) which results in protonation of D85 ($\vartheta_{\text{D85}} \rightarrow 1$)

The equilibrium distribution of the protons between X and D85 (the corresponding amounts are defined as BR_{D85} and BR_X, respectively) can be given by:

$$BR_{D85} = \vartheta_X(1 - \vartheta_{D85})BR_X \exp\left(-\frac{W_A}{kT}\right), \tag{9}$$

where W_A is the energy difference for the proton at X and D85, respectively. If both states are protonated, the occupation factors: $\vartheta_{\text{D85}} = \vartheta_X = 1$, and then the relationship according to Eq. 9 is inappropriate. Under the normal conditions $\vartheta_{\text{D85}} = 0$ and $\vartheta_X = 1$, the amount of protons at BR_X equals to the amounts of the BR molecules in the sample ($\text{BR}_X = \text{BR}$).

As it was already mentioned, the activation energy can be diminished by the external electric field, i.e. $W_A \rightarrow W_A - \Delta W_A$. In the case, when this effect of the external electric field is low, i.e. when $\frac{\Delta W_A}{kT}$ the amount of BR with protonated D85 can be defined from Eq. 9 accordingly:

$$\text{BR}_{\text{AE}} = \text{BR}_{\uparrow\uparrow\downarrow}\exp\left(-\frac{W_A}{kT}\right) \cdot \frac{\Delta W_A}{kT}, \tag{10}$$

where $\text{BR}_{\uparrow\uparrow\downarrow} = \text{BR}_X$ and BR_{AE} determines the amount of the ''acidic'' BR, i.e. subscript ''AE'' indicates the ''acidification'' by the electric field. As a result of the external electric field, ΔpK_a between D85 and X diminishes (via the ΔW_A value). The model presented above describes the proton transfer process in a single BR molecule, but the dried sample consists of a number

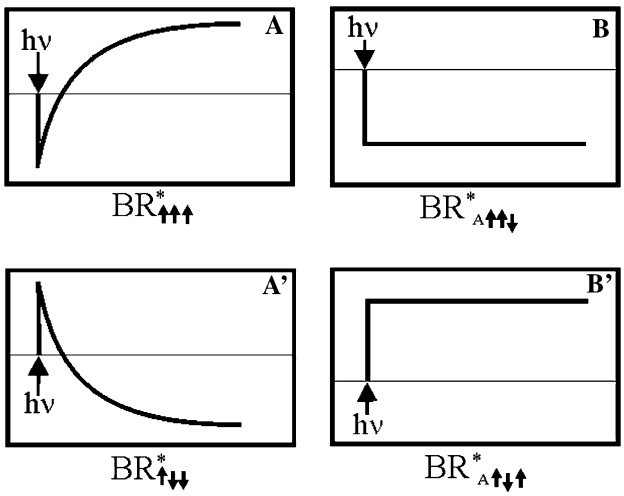

Fig. 6 The shortcuts of the PERSs under different conditions. **Panel a** indicates the normal PERS (according to Eq. 7) of the excited molecules $BR^*_{\uparrow\uparrow\uparrow}$ where the proton pumping direction coincides with the measuring direction and the EEF direction. The *first index arrow* indicates the measuring direction, the *second arrow* corresponds to the direction of the proton pumping and the *third arrow* represents the direction of the EEF. The measuring direction is taken to be from the ITO (ground) electrode towards the metal electrode (see Fig. 1 for details). D85 is protonated in the molecules indicated as $BR^*_{A\uparrow\uparrow\downarrow}$ by the field if the EEF is opposite oriented, subsequently the PERS of such molecules corresponds to Eq. 8 (**panel b**). The molecules where the pumping direction is of the opposite orientation to the measuring direction but coincides with the EEF direction ($BR^*_{\uparrow\downarrow\downarrow}$) produce the normal but inverted PERS (**panel a′**). Finally the molecules where the pumping direction is opposite oriented to the measuring and EEF directions ($BR^*_{A\uparrow\downarrow\uparrow}$) turn to be blocked (D85 is protonated) and the resultant PERS is presented in **panel B′**

of differently oriented BR molecules. The EEF acts vectorially in the molecule, therefore, the direction of the EEF in respect of BR in the PM films should be taken into account. Thus, three main directional factors are playing the predominant role: (1) the measurement direction of the potential, which is considered to be from ITO to the metal electrode; (2) the active proton pumping direction of the individual molecule (the orientation of the molecule); (3) the direction of the external electric field. A detailed schematic representation of differently oriented molecules and the resultant electric potentials for normal and acidic (D85 is protonated) cases is presented in Fig. 6. Thus, $BR_{\uparrow\uparrow\downarrow}$ in Eq. 10 means that the EEF direction is pointing from X to the D85 and therefore the latter can be protonated.

Since we relate the changes of the activation energy ΔW_A to the EEF, it can be defined as follows:

$$\Delta W_A = \delta e U_0, \tag{11}$$

where e is the unit charge, δ is a dimensionless factor, which determines the portion of the potential U_0 for the barrier of a single molecule defining the change of the value of the activation energy. By using Eqs. 10 and 11, the following relationship can be obtained:

$$BR_{AE} = BR_{\uparrow\uparrow\downarrow}\gamma U_0, \tag{12}$$

where

$$\gamma = \frac{e\delta}{kT}\exp\left(-\frac{W_A}{kT}\right). \tag{13}$$

The δ value can be obtained theoretically from the exact calculations of ΔpK_a between D85 and X; however, it is a complicated way. Therefore, we will use the empirical approach by estimating the γ value from fitting the experimental results.

Non-oriented films Let us consider the situation of two molecular layers of the opposite orientations as shown in Fig. 7. The shortcuts of the PERS in particular cases coincide with those presented in Fig. 6. The negative potential is applied to the metal electrode as shown in Fig. 7a. In this case the potential has influence on the lower molecular layer, where the amount of BR molecules, $BR_{A\uparrow\downarrow\uparrow}$, turns out into the ''acidic'' state with the blocked proton transfer. The opposite situation, when the positive potential is applied to the metal electrode, is shown in Fig. 7b. In this case the ''acidification'' takes place in the upper molecular layer. The PERS kinetics in both cases is determined by the decaying exponential with the sign corresponding to the EEF direction. Thus, similarly to the PERS calculations used earlier, we will get:

$$\Delta U_{\text{film}} = \pm k\text{BR}^*\gamma U_0\left[1-\exp\left(-\frac{t}{\tau_L}\right)\right]. \tag{14}$$

Evidently, Eq. 14 is defined by the electrogenicity of the M^+ intermediate and the kinetics reflects the $L \rightarrow M$ transition. The sign in Eq. 14 depends on the EEF direction as follows: $+BR^* = BR^*_{\uparrow\uparrow\downarrow} + BR^*_{\uparrow\downarrow\downarrow}$; and $-BR^* = BR^*_{\uparrow\uparrow\uparrow} + BR^*_{\uparrow\downarrow\uparrow}$. From the experimental results we evaluate: $k\text{BR}^*\ \gamma = 1.2 \times 10^{-3}$. The experimental values of the external potential U_0 are indicated in Fig. 2a. The theoretical PERSs (Fig. 2a, solid lines) calculated according to Eq. 14 well coincide with the experimental observations and with Eq. 1.

Oriented films in the external electric field

Totally oriented films Let us consider two molecular layers in the oriented membranes (see Fig. 8). The shortcuts explaining the PERS of separate BR molecules from each layer are shown schematically in Fig. 6.

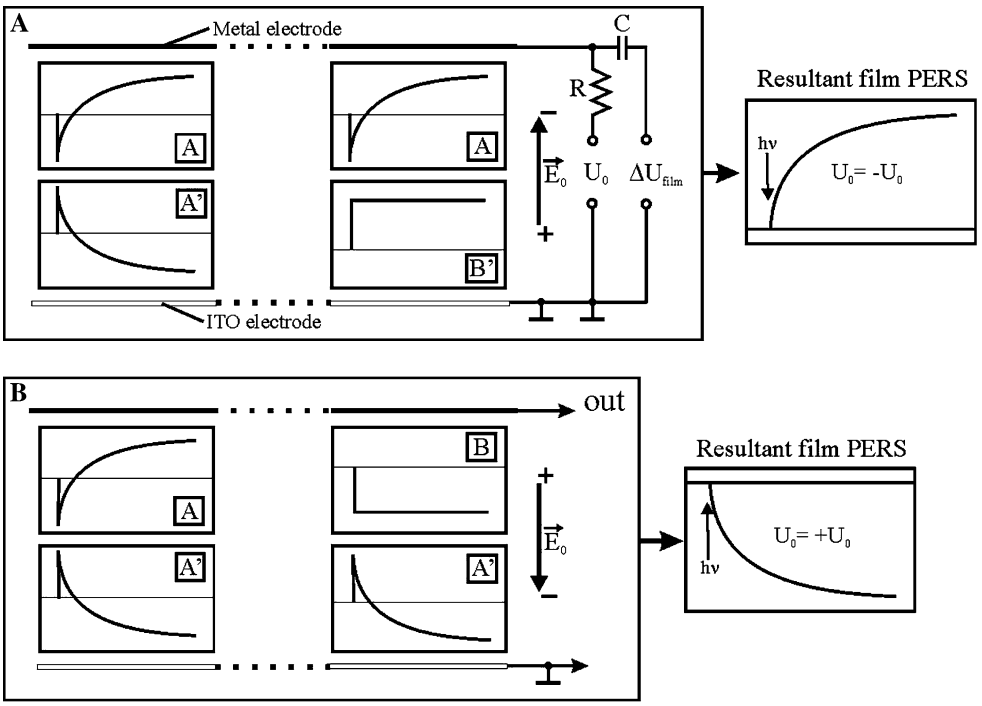

Fig. 7 The non-oriented PM film under the influence of the EEF oriented along the measuring direction (**a**) and of the opposite orientation (**b**). The external electric field is depicted as $\vec{E}_0$. The possible variations of the PERS are depicted as **a**, **b**, **a′** and **b′**, respectively (see Fig. 6 for details). The resultant PERS of such a non-oriented PM film is the superposition (the resultant panel on the *right*) of all the BR molecule responses depicted in separate panels. The effect of the EEF is symmetrical in both directions

The EEF orientation coincides with the direction of the proton pumping, while the negative potential U_0 is applied to the metal electrode (Fig. 8a). In this case the protonation of D85 from the external side (by protons from X and/or H_2O cluster) does not occur, therefore, the PERS coincides with the result given by Eq. 7:

$$\Delta U^{N}_{\text{film}} = k\text{BR}^{*}_{\uparrow\uparrow\uparrow}\left[1 - 2\exp\left(-\frac{t}{\tau_L}\right)\right]. \quad (15)$$

In the opposite polarity of the EEF (Fig. 8b) it acts against the proton pumping in accord with the situation shown in Fig. 5, and in some BR molecules (labeled as B) D85 could be protonated. The PERS kinetics in this case behaves as defined by Eq. 8. Thus, by using Eqs. 7 and 8, we will obtain:

$$\Delta U^{\text{N+AE}}_{\text{film}} = k\text{BR}^{*}_{\uparrow\uparrow\downarrow}\left[1 - 2\exp\left(-\frac{t}{\tau_L}\right) - 2\gamma U_0\left(1 - \exp\left(-\frac{t}{\tau_L}\right)\right)\right]. \quad (16)$$

Equation 16 describes the PERS of the totally oriented film where index ''AE'' in the subscript ($\Delta U^{\text{N+AE}}_{\text{film}}$) denotes molecules affected (''acidified'') by the EEF.

Oriented films In reality the film cannot be totally oriented—some non-oriented fraction should still persist. Hence the PERS of an oriented film in the presence of the EEF consists of two components: the resultant potential of the oriented part (Eq. 16) and the potential of the non-oriented part (Eq. 14). The orientation factor α should be defined as $\alpha = \text{BR}_{\uparrow\uparrow}/(\text{BR}_{\uparrow\uparrow} + \text{BR}_{\uparrow\downarrow})$ thus, $\alpha = 0.5 \div 1$. By using this definition we will get:

$$\text{BR}_{\uparrow\uparrow} = \text{BR}(2\alpha - 1), \quad (17)$$

where $\text{BR} = \text{BR}_{\uparrow\uparrow} + \text{BR}_{\uparrow\downarrow}$.

In the case of the totally oriented film α should reach 1. However, for the PERS of the film, which is considered as a mixture of oriented and non-oriented fractions, summing up Eqs. 14 and 15, and taking into account the orientational factor, we will get:

$$\Delta U^{\text{N+AE}}_{\text{film}} = k\text{BR}^{*}\left\{(2\alpha - 1)\left[1 - 2\exp\left(-\frac{t}{\tau_L}\right)\right] - 2\alpha\gamma U_0\left[1 - \exp\left(-\frac{t}{\tau_L}\right)\right]\right\}. \quad (18)$$

Equation 18 describes the situation when the EEF is opposite oriented to the measuring direction, and in the opposite case by using Eqs. 14 and 16 we will get:

$$\Delta U^{\text{N+AE}}_{\text{film}} = k\text{BR}^{*}_{\uparrow\uparrow\uparrow}\left\{(2\alpha - 1)\left[1 - 2\exp\left(-\frac{t}{\tau_L}\right)\right] + 2(\alpha - 1)\gamma U_0\left[1 - \exp\left(-\frac{t}{\tau_L}\right)\right]\right\}. \quad (19)$$

The EEF influence could be diminished by subtracting the PERS at EEF = 0 from the PERS signals at

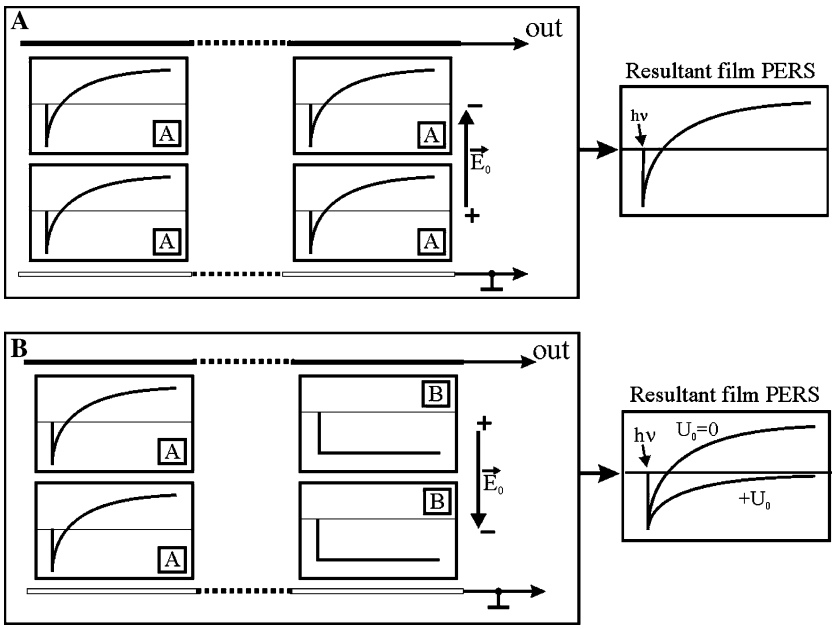

Fig. 8 The oriented PM film under the influence of the EEF oriented along the measuring (and proton pumping) direction (**a**) and of the opposite orientation (**b**). The PERSs of these molecules are ‘ as *A* and *B* (see Fig. 6 for details). The resultant PERS of such a PM film is the superposition (the resultant panel on the *right*) of all the BR molecule responses depicted in separate panels. The external electric field ‘‘blocks’’ the active proton pumping in affected molecules and reduces the second part of the photoresponse if oriented oppositely to the active proton pumping (*B*), while the EEF oriented along the pumping direction does not affect the photoresponse (*A*)

different voltages, thus, obtaining the following relationships:

$$\Delta(\Delta U_{\text{film}}) = -k\text{BR}^{*}_{\uparrow\uparrow\downarrow} 2\alpha\gamma U_0 \left[1 - \exp\left(-\frac{t}{\tau_L}\right)\right], \qquad (20)$$

$$\Delta(\Delta U_{\text{film}}) = k\text{BR}^{*}_{\uparrow\uparrow\uparrow} 2(1-\alpha)\gamma U_0 \left[1 - \exp\left(-\frac{t}{\tau_L}\right)\right]. \qquad (21)$$

The slopes defined as $\theta = \Delta(\Delta U_{\text{film}})/U_0$ for $t \rightarrow \infty$ as follows from Eqs. 20 and 21 are shown in Figs. 2b and 3c. Thus, the orientation factor can be defined accordingly:

$$\frac{tg(\theta_1)}{tg(\theta_2)} = \frac{1-\alpha}{\alpha}. \qquad (22)$$

In the case of non-oriented films, $\alpha = 0.5$ and $\theta_1 = \theta_2$, and for the totally oriented films, $\alpha = 1$ and consequently $\theta_1 = 0$. For the oriented film used in our measurements (see Fig. 3) the orientation factor $\alpha = 0.647$ was obtained. Since $2(\alpha - 1) = 0.3$, hence approximately 30% of the PM membranes were oriented in our sample. According to this assumption the totally oriented film should produce the PERS of 8 V.

According to our model the EEF vectorially changes the pK_a value of the active residues in BR. The EEF oriented along the proton pumping direction does not affect the active proton pumping, while in the opposite orientation it initiates the protonation of the acceptor D85. The above analysis demonstrates that the non-oriented films could also be used in the electrical studies of the BR pump. Accordingly, the orientation degree of the BR film under the influence of the EEF could be evaluated. It is noteworthy that the same effect caused by orientation as defined by Eq. 22 is also observable in flash-photolysis measurements (not shown).

Acknowledgments Authors B.P.K., P.S. and L.V. are grateful to the Lithuanian State Science and Studies Foundation and G.V. is grateful to the National Science Research Fund of Hungary OTKA T048706 for the financial support of this work.

References

Balashov SP, Govindjee R, Imasheva ES, Misra S, Ebrey TG, Feng Y, Crouch RK, Menick DR (1995) The two pKa’s of aspartate-85 and control of thermal isomerization and proton release in the arginine-82 to lysine mutant of bacteriorhodopsin. Biochemistry 34(27):8820–8834

Balashov SP, Imasheva ES, Govindjee R, Ebrey TG (1996) Titration of Aspartate-85 in bacteriorhodopsin: what it says

about chromophore isomerization and proton release. biophys J 70:473–481
Bamberg E, Dencher NA, Fahr A, Heyn MP (1980) Transmembraneous incorporation of photoelectrically active bacteriorhodopsin in planar lipid bilayers. Proc Natl Acad Sci USA 78:7502–7506
Belrhali E, Nollert P, Royant D, Menzel C, Rozenbusch JR, Landau E. Pebay-Peyroula (1999) Protein, lipid and water organization in bacteriorhodopsin: a molecular view of the purple membrane at 1.9 angstroms resolution. Structure 7:909–917
Braun D, Dencher NA, Fahr A, Lindau M, Heyn MP (1988) Nonlinear voltage dependence of the light-driven proton pump current of bacteriorhodopsin. Biophys J 53:617–621
Brown LS, Dioumaev AK, Needleman R, Lanyi JK (1998) Connectivity of the retinal Sciff base to Asp85 and Asp96 during the basteriorhodopsin photocycle: the local-access model. Biophys J 75:1455–1465
Brown LS, Needleman R, Lanyi JK (2002) Conformational change of the E–F interhelical loop in the M photointermediate of bacteriorhodopsin. J Mol Biol 317:471–478
Butt HJ, Fendler K, Bamberg E, Tittor J, Oesterhelt D (1989) Aspartic acids 96 and 85 play a central role in the function of bacteriorhodopsin as a proton pump. EMBO J 8:1657–1663
Chamorovsky SK, Lukashev EP, Alexander AA, Kononenko A, Rubin AB (1983) Effects of electric field on the photocycle of bacteriorhodopsin. Biochim Biophys Acta 725:403–406
Chang CH, Chen JG, Govindjee R, Ebrey T (1985) Cation binding by bacteriorhodopsin. Proc Natl Acad Sci USA. 82:396–400
Chizmadjev YA, Aityan SK (1977) Ion transport across sodium channels in biological membranes. J Theor Biol 64(3):429–453
Chronister EL, Corcoran TC, Song L, El-Sayed MA (1986) On the molecular mechanism of the Schiff base deprotonation during the bacteriorhodopsin photocycle. Proc Natl Acad Sci USA 83:8580–8584
De Groot HJ, Smith SO, Courtin J, Van den Berg E, Winkel C, Lugtenburg J, Griffin RG, Herzfeld J (1990) Solid-state ^{13}C and ^{15}N NMR study of the low pH forms of bacteriorhodopsin. Biochemistry. 29:6873–6883
Dér A, Hargittai P, Simon J (1985) Time-resolved photoelectric and absorption signals from oriented purple membranes immobilized in gel. J Biochem Biophys Methods 10:295–300
Drachev LA, Kaulen AD, Skulachev VP (1978) Time resolution of the intermediate steps in the bacteriorhodopsin-linked electrogenesis. FEBS Lett 87:161–167
Edman K, Royant A, Larsson G, Jacobson F, Taylor T, van der Spoel D, Landau EM, Peyroula EP, Neutze R (2004) Deformation of helix C in the low temperature L-intermediate of bacteriorhodopsin. J Biol Chem 279:2147–2158
Essen LO, Siegert R, Lehmann WD, Oesterhelt D (1998) Lipid patches in membrane protein oligomers: crystal structure of the bacteriorhodopsin–lipid complex. Proc Natl Acad Sci USA. 95:11673–11678
Fischer U, Oesterhelt D (1979) Chromophore equilibriums in bacteriorhodopsin. Biophys J 28:211–230
Gergely C, Zimányi L, Váró G (1997) Bacteriorhodopsin intermediate spectra determined over wide pH range. J Phys Chem B 101:9390–9395
Groma GI, Kelemen L, Kulcsar A, Lakatos M, Váró G (2001) Photocycle of dried acid form of bacteriorhodopsin. Biophys J 81:3432–3441
Grudinin S, Buldt G, Gordeliy V, Baumgaertner A (2005) Water molecules and hydrogen-bonded networks in bacteriorhodopsin—molecular dynamics simulations of the ground state and the M-intermediate. Biophys J 88:3252–3261
Hellingwerf KJ, Schuurmans JJ, Westerhoff HV (1978) Demonstration of coupling between the protonmotive force across bacteriorhodopsin and the flow through its photochemical cycle. FEBS Lett 92:181–186
Hong FT, Montal M (1979) Bacteriorhodopsin in model membranes, a component of the displacement photocurrent in the microsecond time scale. Biophys J 25:465–472
Imasheva ES, Balashov SP, Ebrey TG, Chen N, Crouch RK, Menick DR (1999) Two groups control light-induced schiff base deprotonation and the proton affinity of Asp85 in the Arg82his mutant of bacteriorhodopsin. Biophys J 77:2750–2763
Kandori H (2004) Hydration switch model for the proton transfer in the Schiff base region of bacteriorhodopsin. Biochim Biophys Acta 1658:72–79
Kietis P, Vengris M, Valkunas L (2001a) Electrical-to-mechanical coupling in purple membranes: membrane as electrostrictive medium. Biophys J 80:1631–1640
Kietis P, Vengris M, Valkunas L (2001b) In: Der A, Keszthelyi L (eds) Bioelectronic applications of photochromic pigments. NATO science series, IOS Press, Amsterdam, pp 185–197
Kietis P, Linge D, Saudargas P, Valkunas L (2001c) Photoelectric response and electrostrictive properties of dried purple membrane films: the comparative study. Lith J Phys 41:477–483
Kietis PB, Saudargas P, Valkunas L (2002) Electrostriction of purple membranes and the model of active proton transfer in bacteriorhodopsin. SPIE Proc 5122:122–131
Kietis PB, Saudargas P, Valkunas L (2005) Piezoelectric model for active proton transport in bacteriorhodopsin. Lith J Phys 45:397–409
Kimura Y, Vassylyev DG, Miyazawa A, Kidera A, Matsushima M, Mitsuika K, Murata K, Hirai T, Fujiyoshi Y (1997) Surface of bacteriorhodopsin revealed by high-resolution electron crystallography. Nature 389:206–211
Kobayashi T, Ohtani H, Iwai JI, Ikegami A, Uchiki H (1983) Effect of pH on the photoreaction cycles of bacteriorhodopsin. FEBS Lett 162:197–200
Kolodner P, Lukashev EP, Ching YC, Rousseau D (1996) Electric-field-induced Schiff base deprotonation in D85N mutant bacteriorhodopsin. Proc Natl Acad Sci USA 93:11618–11621
Kolodner P, Lukashev EP, Ching YC, Rousseau D, Sheves M (1999) Electric-field effects in 13-demethyl-11,14-epoxyretinal-bacteriorhodopsin films. Photochem Photobiol 70:103–110
Kolodner P, Lukashev EP, Ching Y (2000) Electric-field effects in dry films of D85N and D8596N mutant bacteriorhodopsin. Bioelectrochemistry 51:67–73
Lanyi JK (1993) Proton translocation mechanism and energetics in the light-driven pump bacteriorhodopsin. Biochim Biophys Acta Bioenerg 1183:241–261
Lanyi JK (2000a) Molecular mechanism of ion transport in bacteriorhodopsin: insights from crystallographic, spectroscopic and mutational studies, J Phys Chem B 104:11441–11448
Lanyi JK (2000b) Bacteriorhodopsin: a special issue. Biochim Biophys Acta 1460:1–239
Lanyi JK (2004a) X-ray diffraction of bacteriorhodopsin photocycle intermediates (Review). Mol Membr Biol 21:143–150
Lanyi JK (2004b) Bacteriorhodopsin. Annu Rev Physiol 66:665–688

Lanyi JK (2004) What is real crystallographic structure of the L photointermediate of bacteriorhodopsin?. Biochim Biophys Acta 1685:14–22

Lanyi JK, Schobert B (2002) Crystallographic structure of the retinal and the protein after deprotonation of the schiff base: the switch in the bacteriorhodopsin photocycle. J Mol Biol 321:727–737

Lanyi KL, Schobert B (2003) Mechanizm of proton transport in bacteriorhodopsin from crystallographic structures of the K, L, M_1, M_2, and M_2' intermediates of the photocycle. J Mol Biol 328:439–450

Läuger P, Benz R, Stark G, Bamberg E, Jordan PC, Fahr A, Brock W (1981) Relaxation studies of ion transport systems in lipid bilayer membranes. Q Rev Biophys 14:513–598

Ludmann K, Gergely C, Der A, Váró G (1998) Electric signals during the bacteriorhodopsin photocycle, determined over a wide pH range. Biophys J 75:3120–3126

Luecke H, Schobert B, Richter HT, Cartailler JP, Lanyi JK (1999a) Structural changes in the M photointermediate of bacteriorhodopsin at 2 angstrom resolution. Science 286:255–260***

Luecke H, Schobert B, Richter HT, Cartailler JP, Lanyi JK (1999b) Structure of bacteriorhodopsin at 1.55 A resolution. J Mol Biol 291:899–911***

Lukashev EP, Vozary E, Kononenko AA, Rubin AB(1980) Electric field promotion of the bacteriorhodopsin BR_{570} to BR_{412} photoconversion in films of *Halobacterium halobium* purple membranes. Biochim Biophys Acta 592:258–266

Lukashev EP, Vozary E, Kononenko AA, Rubin AB, Abdulaev NG (1982) Electric field regulation of bacteriorhodopsin photochromic cycle (in russian). Bioorg Chem 8:1173–1179

Lukashev EP, N. Kh. Seifullina, Kolodner P (2001) Effect of the external electric field on the formation of M-product in oriented bacteriorhodopsin films (in Russian). Biol Membr 18:137–144

Mathies RA, Lin SW, Ames JB, Pollard WT (1991) From femtoseconds to biology: mechanism of bacteriorhodopsin's light-driven proton pump, Annu Rev Biophys Biophys Chem 20:491–518

Metz G, Siebert F, Engelhard M (1992) Asp85 is the only internal aspartic acid that gets protonated in the M intermediate and the purple-to-blue transition of bacteriorhodopsin. FEBS 303:237–241

Mowery PC, Lozier RH, Chae Q, Tseng YW, Taylor M, Stoeckenius W (1979) Effect of acid pH on the absorption spectra and photoreactions of bacteriorhodopsin. Biochemistry 18:4100–4107

Neutze R, Peyroula EP, Edman K, Royant A, Navarro J, Landau EM (2002) Bacteriorhodopsin: a high-resolution structural view of vectorial proton transport. Biochim Biophys Acta 1565:144–167

Oesterhelt D, Stoeckenius W (1973) Functions of a new photoreceptor membrane. Proc Natl Acad Sci USA 70:2853–2857

Ohtani H, Kobayashi T, Iwai JI, Ikegami A (1986) Picosecond and nanosecond spectroscopies of the photochemical cycles of acidified bacteriorhodopsin. Biochemistry 25:3356–3363

Rotschild KJ (1992) FTIR difference spectroscopy of bacteriorhodopsin: toward a molecular model. J Bioenerg Biomembr 24:147–167

Rousso I, Khatchatryan E, Brodsky I, Nachustai R, Ottolenghi M, Sheves M, Lewis A (1997) Atomic force sensing of light-induced protein dynamics with microsecond time resolution in bacteriorhodopsin and photosynthetic reaction centres. J Struct Biol 119:158–164

Schobert B, Vickery JC, Hornak V, Smith SO, Lanyi JK (2002) Crystallographic structure of the K intermediate of bacteriorhodopsin: conservation of free energy after photoisomerization of the retinal. J Mol Biol 321:715–726

Simmeth R, Rayfield GW (1990) Evidence that the photoelectric response of bacteriorhodopsin occurs in less than 5 picoseconds. Biophys J 57:1099–1101

Váró G (1981) Dried oriented purple membrane samples. Acta Biol Acad Sci Hung 32:301–310

Váró G, Keszthelyi L (1983) Photoelectric signals from dried oriented purple membranes of *Halobacterium halobium*. Biophys J 43:47–51

Váró G, L. Keszthelyi (1985) Arrhenius parameters of the bacteriorhodopsin photocycle in dried oriented samples. Biophys J 47:243–246

Váró G, Lanyi JK (1989) Photoreactions of bacteriorhodopsin at acid pH. Biophys J 56:1143–1151

Váró G, Lanyi JK (1991) Kinetic and spectroscopic evidence for an irreversible step between deprotonation and reprotonation of the Schiff base in the bacteriorhodopsin photocycle. Biochemistry 30:5008–5015

Wang J (2000) Photocurrent from oriented membrane films containing acid-blue and acid-purple bacteriorhodopsin and its mutants. Photochem Photobiol 71(4):476–480

Zhu F, Schulten K (2003) Water and proton conduction through carbon nanotubes as models for biological channels. Biophys J 85:236–244